LIQUEFACTION AND SOIL FAILURE DURING 1994 NORTHRIDGE EARTHQUAKE

By Thomas L. Holzer,[1] Michael J. Bennett,[2] Daniel J. Ponti,[3] and John C. Tinsley III[4]

ABSTRACT: The 1994 Northridge, Calif., earthquake caused widespread permanent ground deformation on the gently sloping alluvial fan surface of the San Fernando Valley. The ground cracks and distributed deformation damaged both pipelines and surface structures. To evaluate the mechanism of soil failure, detailed subsurface investigations were conducted at four sites. Three sites are underlain by saturated sandy silts with low standard penetration test and cone penetration test values. These soils are similar to those that liquefied during the 1971 San Fernando earthquake, and are shown by widely used empirical relationships to be susceptible to liquefaction. The remaining site is underlain by saturated clay whose undrained shear strength is approximately half the value of the earthquake-induced shear stress at this location. This study demonstrates that the heterogeneous nature of alluvial fan sediments in combination with variations in the ground-water table can be responsible for complex patterns of permanent ground deformation. It may also help to explain some of the spatial variability of strong ground motion observed during the 1994 earthquake.

INTRODUCTION

The Northridge, California, earthquake (**M** = 6.7; M_s = 6.8) of January 17, 1994 was the most costly earthquake ever to strike the United States. It was also the largest earthquake to occur in the Los Angeles metropolitan area since the 1971 San Fernando Valley (**M** = 6.6) earthquake (''The magnitude'' 1994). Estimated property losses ranged from $20 to $30 billion. Although ground shaking directly caused most of the earthquake damage, permanent ground deformation locally caused significant damage to pipelines, sewers, and surface structures. Ground failures ranged from slope failures in the mountains to ground cracking in alluvium-filled valleys (''USGS'' 1996). The earthquake, which was associated with a blind reverse fault, did not produce primary surface faulting.

Permanent ground deformation in alluvium underlying the gently sloping valley floor of the San Fernando Valley was particularly enigmatic. Although ground cracks and distributed permanent ground deformation severely damaged buried utilities and foundations of structures (O'Rourke et al. 1996; O'Rourke and Toprak 1997), the specific mechanism of failure at many sites was unclear. Cracks formed on gently sloping ground remote from free faces or known areas of cut and fill. Most failures were not accompanied by sand boils, indicative of liquefaction. The general absence of sand boils prompted diverse speculation about the mechanism of failure. Proposed causes of failure ranged from coseismic faulting on nonseismogenic faults (Cruikshank et al. 1996; Johnson et al. 1996) to localized shallow soil failure caused by ground shaking (Holzer et al. 1996; Stewart et al. 1996). To resolve this ambiguity, detailed geotechnical investigations were conducted to determine subsurface conditions at selected sites where permanent ground deformation was observed. The writers conclude that soil failure was caused primarily by liquefaction of silty sand, although dynamic failure of lean clay is indicated at one site.

The present paper updates the work of Holzer et al. (1996), which presented preliminary conclusions, with additional data and analysis. Complete geotechnical data, including boring logs, on which the present paper is based are available in Bennett et al. (1998).

METHOD OF STUDY

Detailed subsurface investigations were conducted at four sites to determine both geotechnical properties of shallow materials and geologic structure (Fig. 1). Three sites are in the San Fernando Valley near the 1994 earthquake epicenter; their locations range from the margin of the valley to the gently sloping valley floor. The fourth site, Potrero Canyon, is a narrow sediment-filled valley located 22 km north of the epicentral region. All three San Fernando Valley sites experienced levels of horizontal ground acceleration $\geq 0.5g$; Potrero Canyon experienced slightly lower shaking, $\geq 0.3g$ (Chang et al. 1996). The four sites were selected primarily because both foundations and buried utilities were damaged, and U.S. Geological Survey investigators had carefully documented patterns of ground deformation during postearthquake investigations.

Each site was explored by establishing approximately linear arrays of 15–20 m deep cone penetration test (CPT) soundings and hollow-stem auger borings across the zone of ground failure. Access was generally limited to streets. CPTs were conducted first to define local soil units, and then standard penetration tests (SPTs) and Shelby tube sampling were conducted in nearby auger borings to confirm texture and to characterize geotechnical properties of soil units. In general, SPTs were conducted in material that was suspected to be susceptible to liquefaction on the basis of CPT measurements. Sixty-two CPT soundings and 29 auger borings for SPT measurements were performed. In addition to penetration tests and Shelby tube sampling, in-situ shear strengths were measured to depths of 6 m with a 19 mm field shear vane and shallow ground water was monitored with piezometers. The vane was rotated at 90°/min, which is much higher than the 6°/min rate recommended for field vanes by ASTM D 2573 (*Standard* 1993). Although the vane shear did not impose a cyclic load, it was felt that the higher rotation rate produced a better measure of the dynamic strength of the soil. Shear failure during vane testing occurred in about 20–40 s, which is slightly longer than the approximately 10 s duration of strong shaking (>0.1g) in the epicentral region.

[1]Engrg. Geologist, U.S. Geological Survey, 345 Middlefield Rd., MS 977, Menlo Park, CA 94025. E-mail: tholzer@usgs.gov

[2]Operational Geologist, U.S. Geological Survey, 345 Middlefield Rd., MS 977, Menlo Park, CA.

[3]Res. Geologist, U.S. Geological Survey, 345 Middlefield Rd., MS 977, Menlo Park, CA.

[4]Res. Geologist, U.S. Geological Survey, 345 Middlefield Rd., MS 977, Menlo Park, CA.

Note. Discussion open until November 1, 1999. To extend the closing date one month, a written request must be filed with the ASCE Manager of Journals. The manuscript for this paper was submitted for review and possible publication on March 12, 1998. This paper is part of the ***Journal of Geotechnical and Geoenvironmental Engineering***, Vol. 125, No. 6, June, 1999. ©ASCE, ISSN 1090-0241/99/0006-0438–0452/$8.00 + $.50 per page. Paper No. 17861.

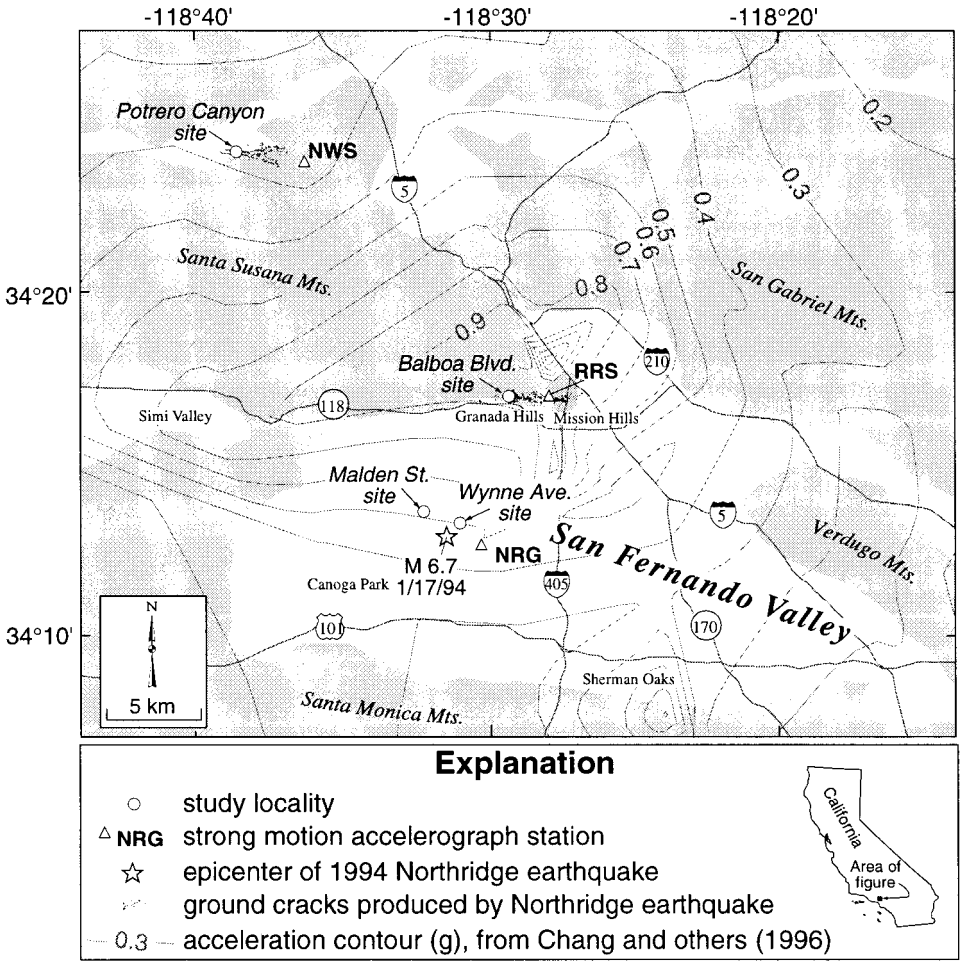

FIG. 1. Map of Sites of Geotechnical Investigation and Strong Motion Recording Stations; Ground Motion Contours Are from Chang et al. (1996)

REGIONAL GEOLOGICAL SETTING

The San Fernando Valley is a structural valley in southern California, which is filled with up to 4,500 m of Tertiary sedimentary rock and alluvial sediment (Wentworth and Yerkes 1971). Holocene age (<10,000 yr) alluvial gravels, sands, and finer sediment with an aggregate thickness ranging from about 8 to 12 m immediately underlie the gently sloping valley floor. This alluvium was deposited by sediment-laden floodwaters that flowed out of the surrounding mountain canyons. Before modern flood control efforts began in the 1920s, extensive valley-wide flooding occurred about every 5 yr. The texture of the Holocene sediment is primarily determined by its source material in the surrounding mountains. At the four study sites, fine-grained Cenozoic and Mesozoic strata are the principal source rocks. In general, Holocene materials rest on either late Pleistocene alluvium of Saugus Formation, which, in the study area, consists of slightly indurated fluvial sediment of late-Pliocene to mid-Pleistocene age. Some of the material identified as Holocene may be slightly older than 10,000 yr; deposition rates increased markedly in the San Fernando Valley when regional climatic conditions shifted from pluvial to semiarid slightly before the formal beginning of the Holocene epoch.

DESCRIPTION OF STUDY SITES

Balboa Boulevard

The Balboa Boulevard site is on the northern margin of the San Fernando Valley, where a 5 km long complex belt of ground cracks formed in the Granada and Mission Hills (Hecker et al. 1995). These cracks were the most areally extensive and damaging ground failure to occur during the Northridge earthquake. Both buried utilities and foundations were damaged. Ground cracks in most of the belt developed in Holocene alluvium on a gentle south-sloping surface. Many cracks in the eastern third of the belt, however, formed on steep slopes in Miocene and Pliocene marine sediment and Pleistocene alluvium, which is exposed at the surface.

The present investigation concentrated on a 1 km long by 0.5 km wide zone of permanent ground deformation at the western end of the 5 km long belt of ground cracks. Cracking in the western zone was generally perpendicular to the 1.6% southern regional topographic gradient, and was more systematic than elsewhere in the 5 km long belt. Displacements across cracks defining the northern margin of the deformation zone indicated failure was by extension, whereas displacements across cracks along the southern margin of the zone indicated failure was by compression. Aggregate displacements across the northern and southern margins of the failure zone were each about 0.5 m as computed from street centerline surveys. Horizontal displacements across individual cracks were small, less than a few centimeters.

Subsurface exploration was conducted along a north-south (NS) 570 m long line in an unnamed alley, 40 m west of Balboa Boulevard [Fig. 2(a)]. The site is underlain by Holocene silty sand to lean clay that ranges in thickness from approximately 8 to 10 m [units A, B, and C, Fig. 2(b)]. The uppermost unit, A, is less than 1 m thick, and consists of fill and reworked sandy silt and lean clay with sand. The upper part of the primary Holocene section, unit B, consists of sheet flood and debris flow deposits; the lower part, unit C, consists

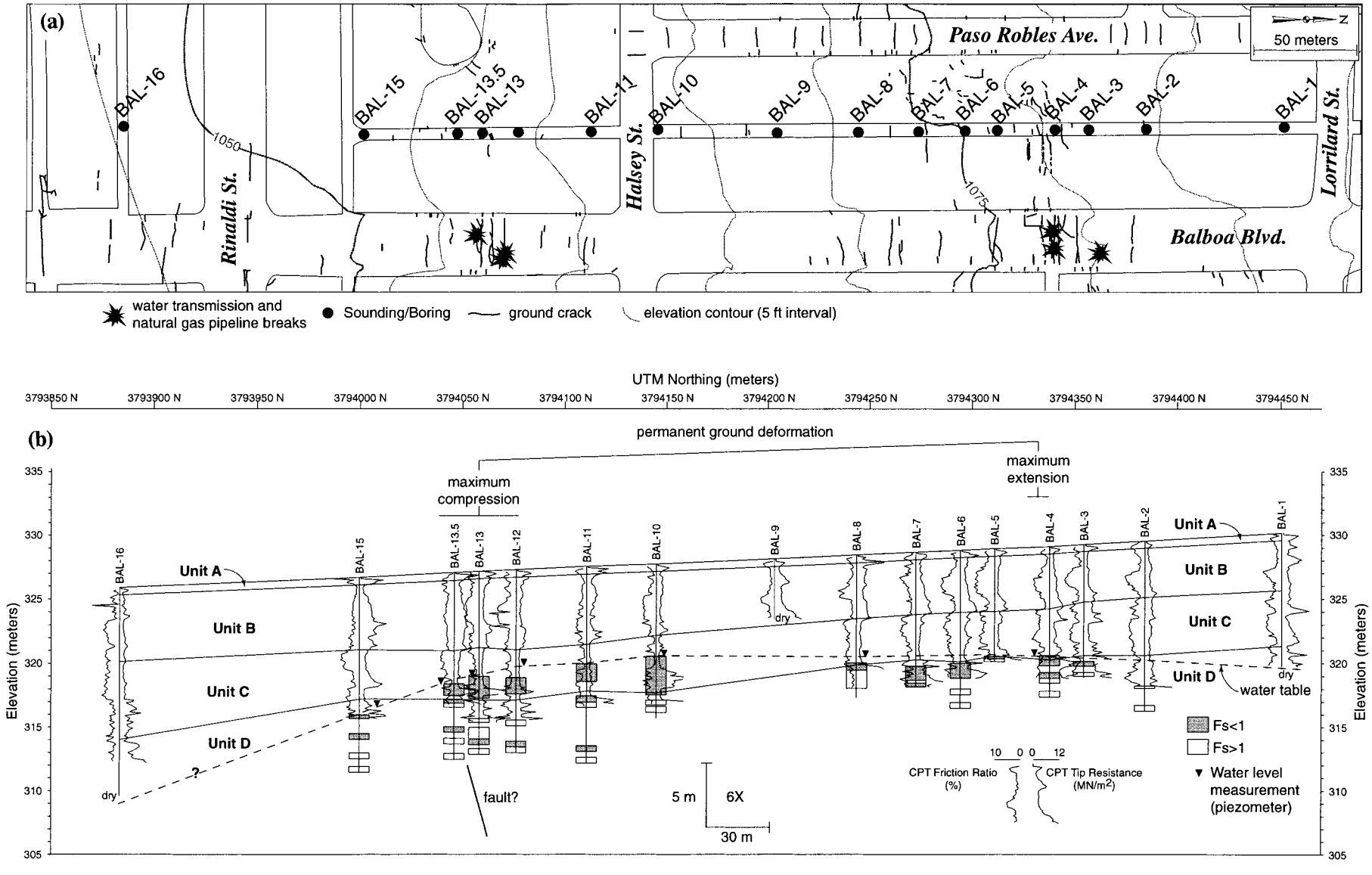

FIG. 2. Map of: (a) Ground Cracks, Major Pipeline Breaks, and Location of Cross Section at Balboa Boulevard Site; (b) Subsurface Cross Section across Failure Zone Showing Soil Units, CPT Soundings, and Liquefaction-Susceptible Intervals of Soil Inferred from CPT and SPT (F_s Is Factor of Safety)

TABLE 1. Engineering Properties of Soil Units (±1σ)

Soil unit (1)	Depth range, m (2)	D_{50} mm (3)	N blows/ft (4)	$(N_1)_{60CS}$ blows/ft (5)	q_{C1CS} MN/m^2 (6)	Fines % <75 μm (7)	Clay % <5 μm (8)	Water content (9)	Atterberg limit PL (10)	Atterberg limit LL (11)	USC (12)
(*a*) Balboa Boulevard											
B	0.8–5.5	0.109	12	—	—	59 ± 16	20 ± 8	17 ± 4	21 ± 2	33 ± 5	CL–SM
C	5.5–10.0	0.083	—	—	—	57 ± 17	19 ± 7	22 ± 5	20 ± 2	32 ± 7	ML/SM
Saturated C	8.0–10.0	0.110	—	21 ± 4	8.3 ± 3.0	52 ± 17	18 ± 8	23 ± 4	19 ± 3	30 ± 8	ML/SM
D	>10.0	0.207	—	59 ± 42	15.0 ± 4.9	48 ± 21	14 ± 9	23 ± 7	22 ± 3	36 ± 9	SM/ML
(*b*) Malden Street											
A	0–2.5	0.019	4	—	—	75 ± 8	31 ± 7	23 ± 6	22 ± 2	35 ± 6	CL
B	2.5–8.5	0.016	7	—	—	80 ± 8	37 ± 10	33 ± 4	22 ± 3	40 ± 6	CL
D	>8.5	0.252	—	43 ± 11	14.4 ± 7.4	43 ± 17	18 ± 10	—	19 ± 1	31 ± 4	SM
(*c*) Wynne Avenue											
A	0–2.5	0.094	8	—	—	51 ± 13	18 ± 6	—	—	—	SM/ML
B	2.5–6	0.027	3	—	—	69 ± 13	26 ± 7	29 ± 5	22 ± 3	38 ± 5	CL–SM
C	6–15.5	0.041	—	—	—	75 ± 20	32 ± 11	30 ± 7	21 ± 3	40 ± 2	CL–ML
C_1	6.0–75	0.153	—	20 ± 6	13.5 ± 5.8	38 ± 23	10 ± 7	24 ± 5	—	—	SM
C_2	10.0–11.5	0.161	—	27 ± 10	17.3 ± 8.9	38 ± 16	12 ± 6	—	—	—	SM
D	>15.5	0.111	—	68	17.7 ± 5.2	38	11	—	—	—	SM
(*d*) Potrero Canyon											
A	2.5–7.0	0.029	2	—	—	78 ± 12	24 ± 9	28 ± 5	24 ± 3	33 ± 5	CL/ML
C	2.5–1.0	0.033	6	—	—	76 ± 12	21 ± 5	26 ± 6	23 ± 3	28 ± 3	CL/ML
C_1	Variable	0.095	—	15 ± 2	12.5 ± 3.3	57 ± 18	11 ± 3	23 ± 4	24 ± 1	29 ± 4	SM/ML
D	>11.0	0.280	—	57 ± 22	18.1 ± 5.7	31 ± 19	7 ± 7	18 ± 2	19 ± 1	24 ± 1	SM

Note: See Figs. 2, 4, 6, and 7 for identification of soil units. D_{50} is median grain size; USC is the Unified Soil Classification system. $(N_1)_{60CS}$ and q_{C1CS} were computed only for material with clay <15% and are equivalent clean sand values. Textural data are for samples from both Shelby tube and SPT.

of fluvial deposits. The most conspicuous stratigraphic horizon is the contact between the Holocene sediment and the underlying Pleistocene silty sand [unit D, Fig. 2(b)], which the writers interpret to be part of the Saugus Formation on the basis of its clast lithologies and carbonate soil development.

Permanent ground deformation at Balboa Boulevard is limited in the profile to an interval where the water table is within Holocene sediment. As illustrated in Fig. 2(b), locations of maximum compression and extension correlate closely with where the water table falls below the base of the Holocene fluvial unit, C. The zone of lateral ground displacement is well marked on its southern and northern margins by surface cracks and deformation features. Depth to ground water in the failure zone ranged from 7.2 to 10.7 m. Only the basal part of unit C (and none of unit B) was below the water table. Maximum saturated thickness of unit C was about 3 m.

Because many water pipes broke and leaked during the earthquake, the writers were concerned that water levels measured in July 1995, about 18 months after the earthquake, did not represent preearthquake conditions. Accordingly, piezometers were installed in seven auger holes. Remeasurement of water levels in March, June, and December 1996 indicated water levels were stable, which suggests the 1995 measurements were representative of preearthquake conditions. In addition to stable water levels, the darker color of saturated sediment indicated reducing conditions, which suggests that the 1995 water levels reflected a long-term hydrologic situation.

Geotechnical properties of units B, C, and D are shown in Table 1. All units are heterogeneous, ranging from clays to silty sands. Both Holocene units, B and C, have average fines (<75 μm) and clay (<5 μm) contents of about 58% and 20%, respectively, as determined from both Shelby tube and SPT samples. The part of unit C that was below the water table has an average fines content of 52% and clay content of 18%, and does not differ materially from the dry part of C. Only eight SPTs could be performed in the part of unit C that was below the water table; four SPT tests had clay contents <15%. For these four tests, the average equivalent clean sand corrected normalized blow count (Youd and Idriss 1997), $(N_1)_{60CS}$, is 21 blows/ft and the average fines content is 42%. In general, the SPTs are texturally biased because they specifically targeted sandy units inferred from CPT logs. Unit D is much coarser grained, but is still very silty. Its average fines content, based on both Shelby tube and SPT samples, is 48%. Forty-four SPTs were performed in unit D, 29 of which had clay contents <15%. The average $(N_1)_{60CS}$ and fines contents of the 29 tests are 59 blows/ft and 36%, respectively.

Hydrogeologic and stratigraphic evidence suggests a pre-1994 fault zone is present at the south end of the profile, although no fault plane was directly observed. Hydrogeologic evidence consists of the abrupt increase in depth to ground water of more than 8.3 m between borings BAL-13.5 and -16 [Fig. 2(b)], which are 160 m apart. The abrupt change in water level is consistent with a fault acting as a ground-water barrier. The primary stratigraphic evidence for a fault is an organic-rich sandy lens on the south end of the profile. It terminates abruptly to the north and may be a sag pond deposit that formed adjacent to a Pleistocene fault scarp. There is also a marked change in clast lithology and a light increase in the thickness of the Holocene material across the suspected fault zone.

Malden Street

Ground failure at the Malden Street site was part of an approximately 0.5 km long east-west (EW) system of cracks that broke sewers and water lines and damaged foundations of several single-family dwellings (Fig. 3). Although cracks at the western and eastern ends of the failure zone showed left-lateral and right-lateral components of offset, respectively, failure at the study site consisted of a 4 m wide down-dropped block. Permanent vertical offset across cracks bounding the down-dropped block at the study site ranged from 100 to 200 mm. The trend of the failure zone was approximately perpendicular to the 1% regional southeastern topographic gradient. The topographic gradient at the study site, however, slopes to the

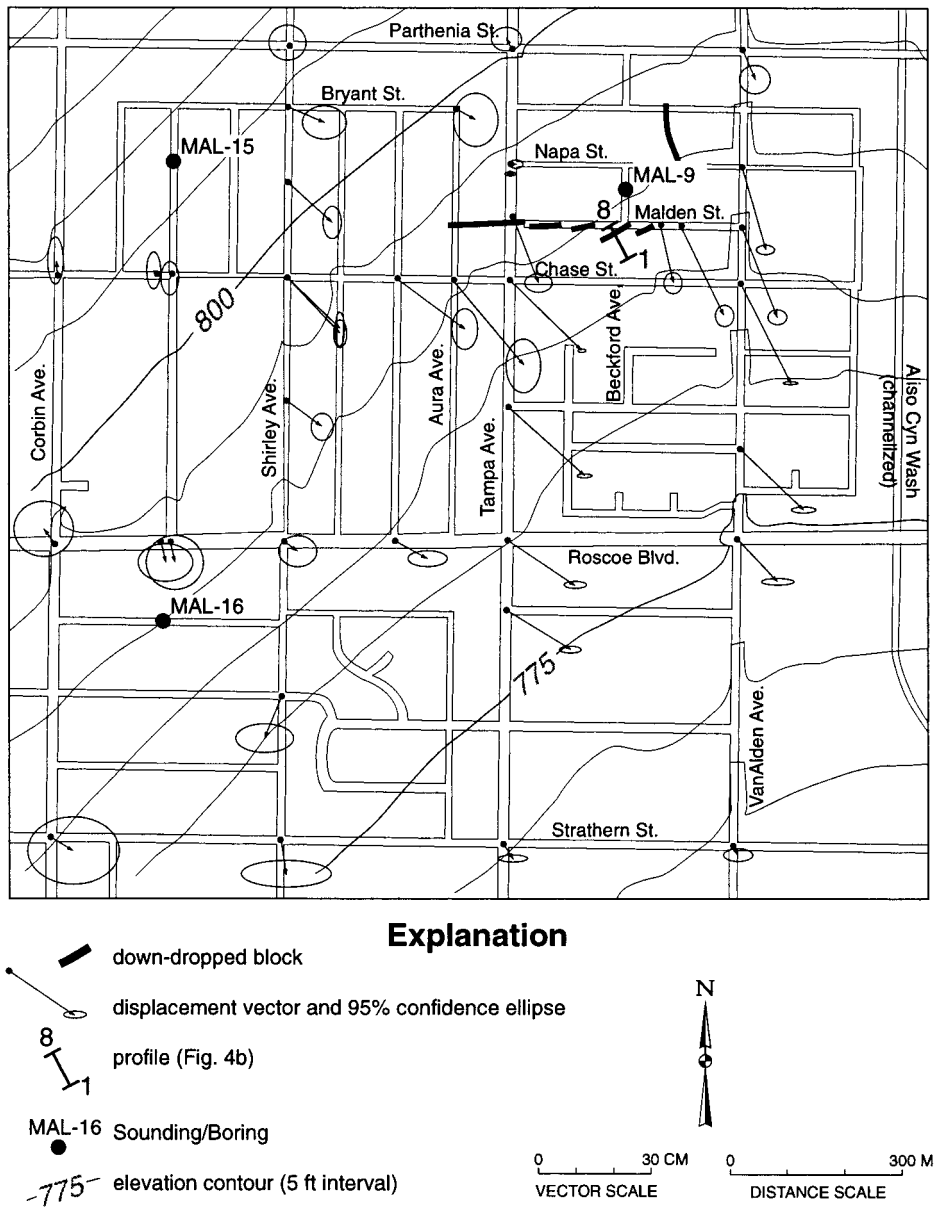

FIG. 3. Horizontal Displacements, Relative to Cluster of Five Survey Points in Northwest Quadrant, near Malden Street; Contours Are Topography Shown in Feet [Figure Modified from Holzer et al. (1996)]

north, having been altered by a 2 m thick blanket of compacted fill [Fig. 4(b)].

The ground cracks mark the northern boundary of a large area that moved southward during the earthquake (Fig. 3). Horizontal displacements near the ground failure were computed from street-centerline surveys conducted before and after the earthquake by the Bureau of Engineering of the City of Los Angeles. Displacements in Fig. 3 are relative to survey points in the northwestern (NW) part of the map. Land south of the zone of cracks moved southeastward 200–300 mm approximately parallel to the topographic gradient. Horizontal tensile strains computed from the displacements were greatest near the cracks, reaching $8{,}000 \times 10^{-6}$ in the direction orthogonal to the average orientation of the cracks [Holzer et al. 1996, Fig. 3(b)]. Extension across the failure zone appears to have been accommodated by distributed compression within an area at least 0.5 km wide southeast (SE) of the cracks.

Subsurface exploration was conducted along a 50 m long NW-SE profile that was perpendicular to the axis of the down-dropped block [Fig. 4(b)]. Two additional borings (MAL-15 and -16) and three CPT soundings (MAL-9, -15, and -16) were conducted within 1 km of the profile (see Fig. 3 for locations). The failure is underlain by 8.5 m of Holocene lean to sandy lean clay [units A and B, Fig. 4(b)]. Ground water beneath the failure zone was at a depth of about 3.9 m and no sands were encountered within the Holocene sediment beneath the water table. The Holocene material includes unit A, a blanket of compacted fill, and unit B, multiple 5–20 cm thick fining upward sequences. Unit B consists of overbank and sheetflood deposits associated with flood events. The most conspicuous stratigraphic marker is the contact between the Holocene clay and upper Pleistocene silty sand, unit D, at a depth of 8.5 m. The contact slopes gently to the southeast in the profile.

The most distinctive textural aspect of the underlying Holocene sediment (see unit B in Table 1) is its fine-grained character. The clay content of most of unit B is greater than 30%, and the fines content is greater than 70%. Its average plasticity index (*PI*) is 18. Clay content of saturated material directly beneath the failure ranges from 22% to 47% and averages 31%.

The part of unit B from 4.3 to 5.8 m beneath the down-dropped block is of particular geotechnical interest. As shown

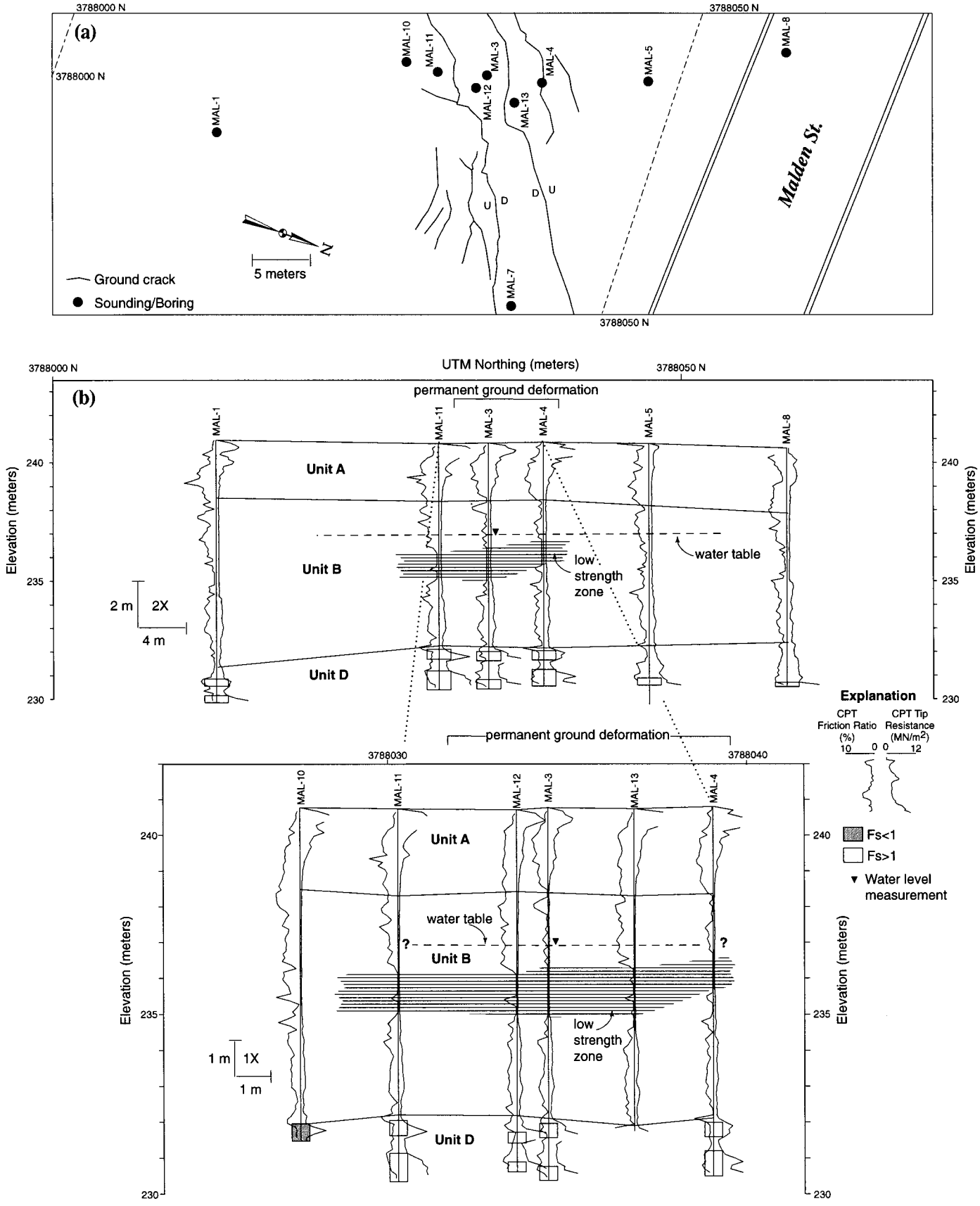

FIG. 4. Map of: Ground Cracks at Malden Street Site; (b) Subsurface Cross Section Showing Soil Units and CPT Soundings

in the soundings at the failure (Fig. 5), this interval has both low average shear strength as determined from in-situ vane shear tests and low CPT tip resistance. In the shear vane sounding, strength of the Holocene sediment decreases abruptly from about 120 kPa in unit A to values less than 50 kPa in unit B. Strength decreases in the low strength zone to an average value of 26 kPa before increasing again to about 100 kPa below the zone. CPT tip resistance of the low strength zone is 0.2 MPa. The average *PI*, 14, of the zone does not significantly differ from that of the surrounding material. The

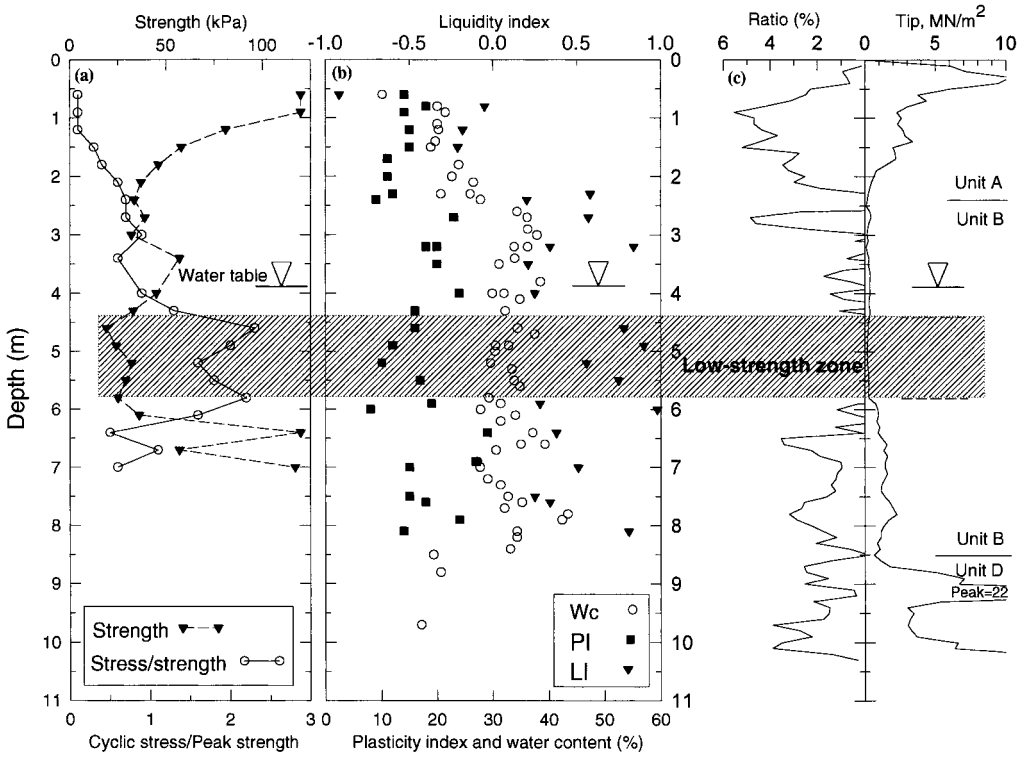

FIG. 5. MAL-3, Malden Street Site (See Fig. 4 for Location: (a) In-Situ Peak Shear Strength and Ratio of Peak Cyclic Shear Stress to In-Situ Peak Shear Strength with Depth; (b) Plasticity and Liquidity Indices (*PI* and *PI*) and water content (W_c); (c) Field Values of CPT Tip Resistance and Friction Ratio

zone can be correlated by CPT laterally and transverse to the down-dropped block over a horizontal distance of only about 10 m [Fig. 4(b)]. An isolated CPT within the down-dropped block, 20 m northeast (NE) of the profile [sounding MAL-7, Fig. 4(a)], indicates that the zone can be correlated laterally and parallel to the ground failure for at least that distance. The zone was 4 m thick in MAL-7, but only about half of it was below the water table. Cultural development prevented systematic exploration of the lateral extent of the zone elsewhere along the failure. A lean clay layer with low tip resistance also was found 1 km SE of the profile (sounding MAL-16, Fig. 3), but that layer was above the water table.

In contrast to the fine-grained Holocene sediment, the underlying Pleistocene sediment is sandy with a D_{50} of 0.25 mm, although parts of it has clay contents >15% (Table 1). Eight SPTs were performed in unit D, of which two had clay content <15%. For these two tests in unit D, and average $(N_1)_{60CS}$ is 43 blows/ft; average fines content is 27%.

Wynne Avenue

Permanent ground deformation at the Wynne Avenue site consisted of an approximately 150 m long by 12 m wide down-dropped block [Fig. 6(a)]. Vertical offset across cracks on Wynne Avenue ranged from 100 to 200 mm. Precise horizontal offsets are unknown, but were comparable in magnitude to the vertical offsets. The axis of the failure zone had a northeast trend that is oblique to the 1.3% south sloping regional topographic gradient. The failure ruptured water lines and sewers.

Nineteen soundings and borings, forming an NS 510 m long profile, were made along the west side of Wynne Avenue both north and south of Cantara Street [Fig. 6(a)]. Ground water beneath the failure zone was at a depth of about 4.3 m. The site is underlain by 2 m of silty sand to sandy lean clay [unit A, Fig. 6(b)], which in turn is underlain by 12–14 m of Holocene sandy silt to lean clay [units B and C, Fig. 6(b)]. Unit B consists of multiple fining upward sequences of overbank and sheetflood deposits that were deposited in a flood basin between major distributary flood channels. Unit C, which is texturally comparable to B, is distinguished by the presence of lenticular sand layers. Immediately beneath the failure, two sand layers are intercalated in unit C at depths of about 6 and 10 m [C_1 and C_2, Figs. 6(b,c)]. The shallower sand layer, C_1, is about 2 m thick. Although it can be traced continuously in the profile, it abruptly becomes siltier south of the failure zone. Its fines content increases from 28% to 44% over a distance of only 4.5 m [see WYN-10 and -11, Fig. 6(b)] beneath the south end of the down-dropped block. The deeper sand layer, C_2, is 1.5 m thick at the failure, but pinches out laterally both north and south of the failure. The most conspicuous stratigraphic contact is between the Holocene sediment and the underlying Pleistocene medium-grained silty sand [unit D, Fig. 6(b)]. The contact is gently sloping in the profile with the exception of a 1.1 m high step beneath the ground failure. The precise declivity of the step is unknown, but it must be fairly steep. It occurs between two soundings, 4 and 5a, which are only 4 m apart. The step is down to the south. Neither layer C_1 nor layer C_2 is offset above the step.

Geotechnical properties of soil units are summarized in Table 1. The uppermost 2 m of unsaturated silty sand to sandy lean clay (unit A) has an average field blow count of 8 blows/ft and a fines content of 51%. The average clay content of the underlying Holocene lean clays (units B and C) is about 28%. The average $(N_1)_{60CS}$ of the two silty sands at 6 and 10 m depths (units C_1 and C_2) is 20 and 27 blows/ft, respectively. Both layers have average fines contents of 38%. Only one SPT was conducted in the Pleistocene silty sand (unit D). It yielded an $(N_1)_{60CS}$ of 68 blows/ft, which is consistent with observed CPT tip resistances.

Potrero Canyon

Potrero Canyon is a narrow 5 km long, EW valley incised into Pliocene sedimentary rock on the north flank of the Santa Susana Mountains. Although it is about 22 km NNW of the

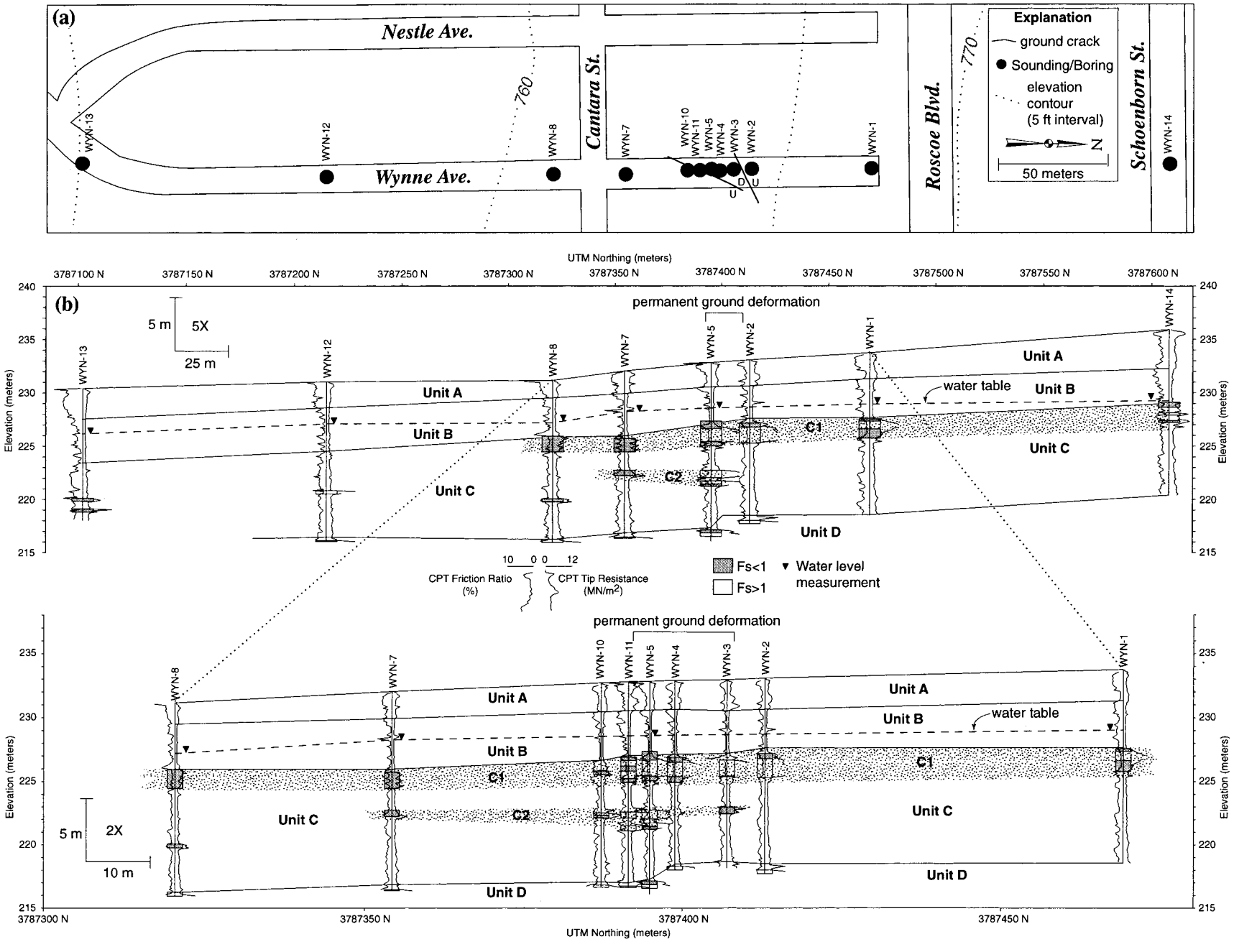

FIG. 6. Map of: (a) Ground Cracks at Wynne Avenue Site; (b) Subsurface Cross Section Showing Soil Units, CPT Soundings, and Liquefaction-Susceptible Intervals of Soil Inferred from CPT and SPT (F_s is factor of Safety)

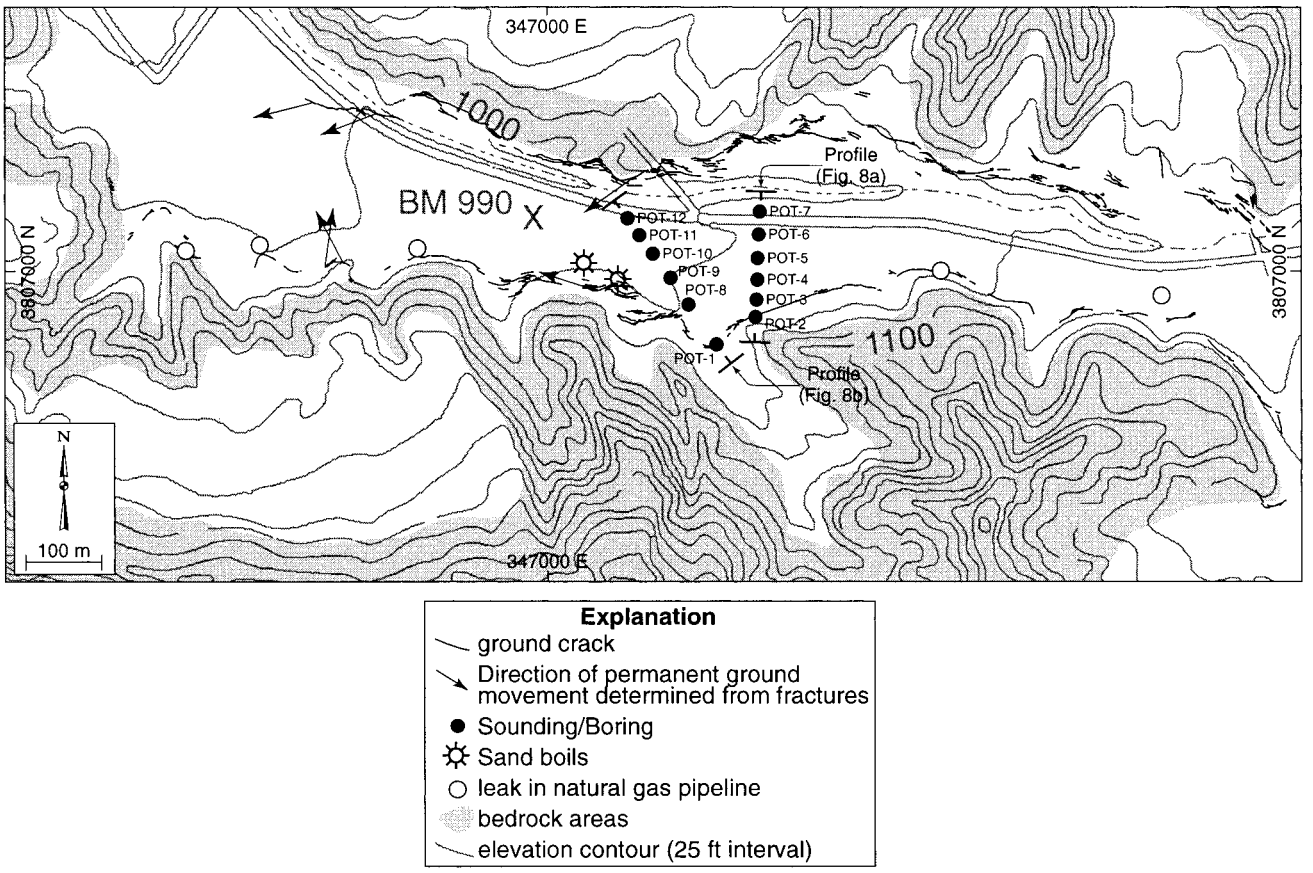

FIG. 7. Map of Ground Cracks, Sand Boils, Gas Transmission Line Breaks, and Geotechnical Sounding Locations at Potrero Canyon; Map Covers Western Half of Failure Zone; Scale Is Shown on Margins of Map

epicenter of the Northridge earthquake, it is near the updip projection of the seismogenic rupture surface.

Ground failure in Potrero Canyon consisted of two zones of ground cracks along the north and south edges of the valley (Fig. 7). Cracks formed in alluvium at or near the contact between the valley fill and the Pliocene bedrock forming the adjacent valley walls (Rymer et al. 1995). Each zone was as much as 30 m wide. Permanent ground deformation was predominantly extensional. Horizontal displacements, inferred from aggregate openings across ground cracks, were at least 10 cm. Vertical components of displacement ranged from a few centimeters to 60 cm. Compressional features, including small thrust faults and broad ridges or mole tracks, were observed on the south side of the valley. These features prompted speculation immediately after the earthquake that the cracking was associated with primary tectonic faulting. Multiple breaks occurred in a 12-in. gas transmission line in the valley (Fig. 7).

A few sand boils vented in the valley (Fig. 7). Most formed on the southern margin of the valley, away from the incised stream that flows near the northern margin of the valley. Sand boils were 1–3 m in diameter and locally coalesced into zones tens of meters long.

Twelve soundings and four borings comprising two profiles, 140 and 207 m long, were performed across Potrero Canyon near the western end of the ground failure (Fig. 7). Each profile spanned the valley. The valley is underlain by fine-grained Holocene sediment, units A and C, (Fig. 8), most of which is below the water table. Depth to ground water was about 2.5 m. The uppermost unit, A, is a homogeneous lean clay to silt with an average thickness of 2.7 m. The remainder of the Holocene section, unit C, consists of lean clay to sand silt with lenses of silt and silty sand, units C_1 (see material susceptible to liquefaction in unit C in Fig. 8). Lenses cannot be unambiguously correlated between adjacent soundings, which averaged 35 m apart. In general, lens thickness is less than 1 m and vertical spacing ranges from 2 to 3 m. Because not all soundings completely penetrated the Holocene section, its maximum total thickness is not known, although it is at least 15 m. A commercial 31 m deep wash boring hole in the valley fill near the profiles encountered materials with field blow counts ≥100 blow/ft at 24 m and siltstone at 29 m (R. T. Frankian and Associates, personal communication, 1997). In addition, a seismic survey coincident with the profile defined by soundings POT-1–POT-12 (Fig. 7) indicates low *P*-wave velocity (<1.0 km/s) sediment extends to a depth of approximately 15 m (Catchings et al. 1998). The Holocene sediment rests on dense silty sand, which may be either Pleistocene or part of the Pliocene Pico Formation (unit D, Fig. 8).

Geotechnical properties of the valley fill are summarized in Table 1. The average $(N_1)_{60CS}$ of the coarser-grained lenses, units C_1, within the Holocene sediment is 15 blows/ft. The average fines content of the lenses is 57% and typically exceeds 35%. Clay contents of these lenses average 11%. Clay contents of units A and C, in which units C_1 are interbedded, typically exceed 15%. Five SPTs were performed in unit D, of which four had clay contents <15%. The average $(N_1)_{60CS}$ is 57 blows/ft for the four tests. The average fines content of unit D is 31%.

POTENTIAL MECHANISMS OF GROUND FAILURE

Liquefaction

Liquefaction Potential

Liquefaction potential was evaluated at all four sites with the simplified procedure of Seed et al. (1985), as modified by Youd and Idriss (1997). Although the original procedure em-

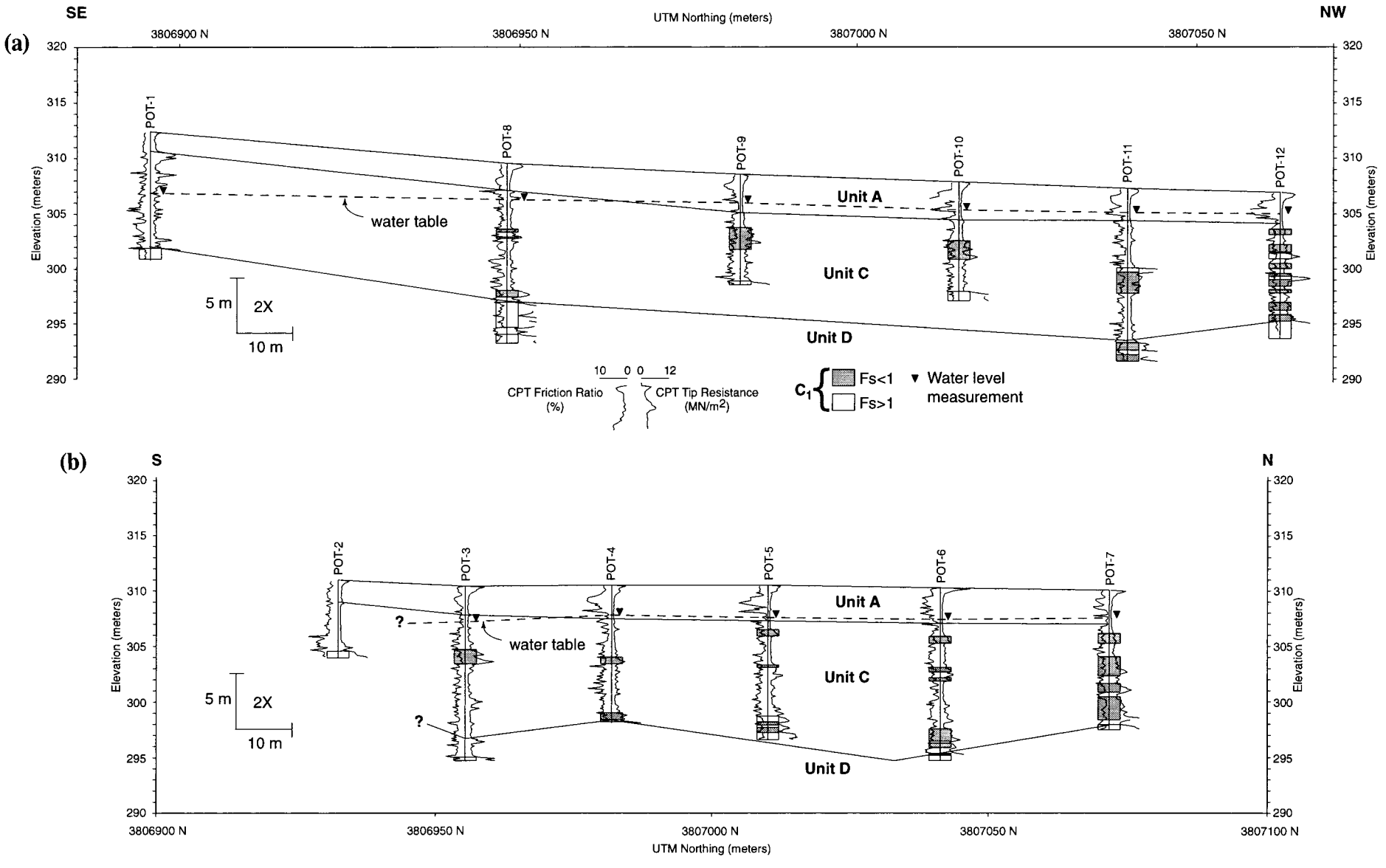

FIG. 8. (a,b) Subsurface Cross Sections through Valley Fill in Potrero Canyon Showing Soil Units, CPT Soundings, and Liquefaction-Susceptible Intervals of Soil (Unit C_1) Inferred from CPT and SPT (F_s Is Factor of Safety); See Fig. 7 for Location of Profiles

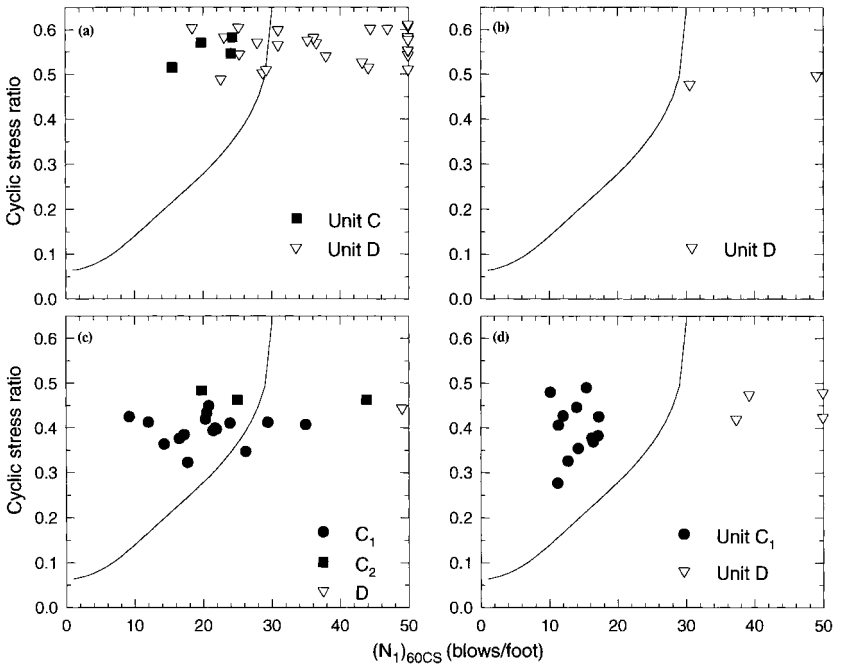

FIG. 9. Liquefaction Potential Based on SPT Blow Counts in Susceptible Holocene and Pleistocene Soil at USGS Study Sites (Youd and Idriss 1997); $(N_1)_{60}$s Were Converted to Equivalent Values for Clean Sand: (a) Balboa Boulevard; (b) Malden Street; (c) Wynne Avenue; (d) Potrero Canyon

phasized SPT blow counts, it has been extended to include CPT measurements as an alternative basis for assessing liquefaction potential. The simplified procedure assumes that only saturated sands with clay contents <15% are susceptible to liquefaction. Per standard practice, field blow counts were normalized to an effective overburden stress of 1 ton/sq ft and corrected for hammer efficiency and rod length; tip resistance also was normalized to 1 ton/sq ft and was corrected for layer thickness. To facilitate the comparison of materials with different fines contents, blow counts and tip resistances were also corrected to equivalent values for clean sand (Youd and Idriss 1997). Equivalent values are indicated by the subscript *CS*.

For the SPT-based liquefaction analysis, there was the concern that thin clayey interbeds might bias estimates of liquefaction potential. Many SPT samples with clay contents <15% were not homogeneous, but included thin interbeds with clay contents >15% within the 12 in. SPT testing interval. The clayey interbeds, which are not liquefiable, reduce the blow count. Because the low blow counts might prompt overestimates of liquefaction potential, SPTs that sampled substantial intervals of interbeds with clay contents >15% were excluded from the analysis.

For the CPT-based analysis, point values of cone resistance measured at 10 cm intervals were used. Use of CPT point values increases the scatter relative to the SPT, which integrates penetration resistance over a 30 cm interval. In each CPT sounding, to avoid undue reliance on isolated values, single or double CPT point values that predicted susceptible material were ignored if they were surrounded by CPT measurements that indicated adjacent material was nonsusceptible. In other words, CPT measurements in a given sounding that indicated clay contents <15% over a 10–20 cm interval were ignored if adjacent CPT measurements indicated the surrounding material had clay contents >15%.

At Balboa Boulevard, all of the SPTs in susceptible Holocene sediment beneath the water table indicate sampled intervals should have liquefied at the intensity of ground shaking experienced during the main shock [Fig. 9(a)]. Values of $(N_1)_{60CS}$ plot well to the left of the boundary between liquefaction and nonliquefaction. In addition to liquefaction of Holocene sediment, some Pleistocene sediment may have liquefied. Seven of the 29 SPTs in the Pleistocene sediment with clay contents <15% yielded factors of safety against liquefaction of less than one. Collectively, however, the Holocene sediment appears to be significantly more liquefiable than the Pleistocene sediment. CPT measurements confirm the SPT measurements, although they suggest that more of the Pleistocene sediment may be liquefiable than do the SPTs [Fig. 10(a)]. Tip resistances of Pleistocene sand, however, plot closer to the nonliquefaction boundary than do Holocene values, indicating a higher factor of safety (F_s). The CPTs also provide insight into the thickness of material that liquefied. In Fig. 2(b), the vertical bars centered on each sounding indicate susceptible material and F_s greater or less than one. The aggregate thickness of liquefied material is inferred to range from 1 to 2 m on the south margin of the lateral spread to less than 1 m on the north margin. The analysis of liquefaction potential used a peak horizontal ground acceleration of 0.84*g*, which was recorded 2.3 km east of the study site at strong motion station RRS (Los Angeles Department of Water and Power Rinaldi Receiving Station, Fig. 1). Other nearby recorded accelerations were as high as 0.94*g*; contoured regional maps of peak acceleration imply a value of 0.85*g* (Chang et al. 1996).

Pipeline deformation in the southern margin of the failure zone beneath Balboa Boulevard is consistent with a liquefaction-induced soil failure. Although permanent offset across the southern margin of the failure zone was compressive, inspection of two ruptured steel gas pipelines—a 22 in. high-pressure transmission and a 6 in. distribution line—indicated that the associated breaks in these lines were subjected to repeated reversals of axial motion, in the range of 150–300 mm or more (R. Gailing, Southern California Gas, personal communication, 1997). This suggests ground oscillation, a phenomenon associated with liquefaction (*Liquefaction* 1985; Pease and O'Rourke 1997), accompanied the lateral spreading.

At Wynne Avenue and Potrero Canyon, the simplified procedure using both SPT and CPT predicts the sand lenses interbedded in the fine-grained Holocene sediment liquefied during the main shock [Figs. 9(c,d) and 10(c,d)]. The remaining Holocene sediment is not considered susceptible to liquefac-

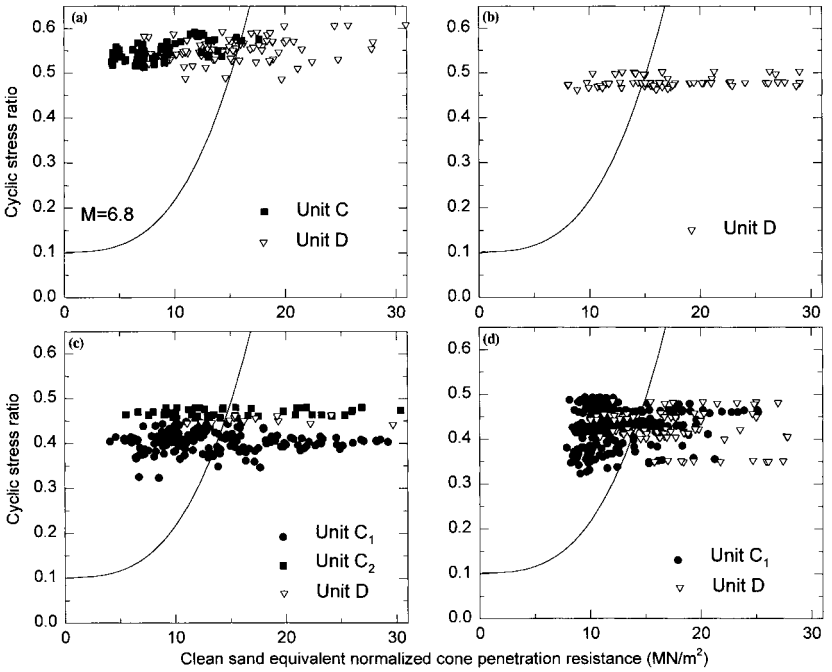

FIG. 10. Liquefaction Potential Based on CPTs in Susceptible Holocene and Pleistocene Soil at Each USGS Study Site (Youd and Idriss 1997); Normalized Tip Resistances Were Converted to Equivalent Values for Clean Sand, q_{c1cs}: (a) Balboa Boulevard; (b) Malden Street; (c) Wynne Avenue; (d) Potrero Canyon

tion by virtue of its >15% clay content. Although none of the SPTs at either site indicates that susceptible Pleistocene sediment liquefied, CPTs indicate some of the Pleistocene sediment may have liquefied.

The intervals at Wynne Avenue where material is inferred from the CPT profiles to have liquefied are shown in Fig. 6. Aggregate thicknesses range from 0.4 to 1.7 m, with most of the liquefied interval occurring in unit C_1. The aggregate thicknesses of liquefied sand beneath the ground failure are not distinctive or anomalous, although it may be noteworthy that the aggregate thickness of susceptible material exceeds 3 m beneath the down-dropped block, whereas elsewhere it is less than 2 m. This suggests the possibility that excess pore pressures generated in only part of the sand layer may have redistributed and reduced the effective stress in nonliquefied portions of the sand layer as well. Intervals where liquefaction is inferred at Potrero Canyon are shown in Fig. 8. Aggregate thicknesses typically are about 2 m, but increase to 5–6 m beneath the north end of the profile. For the liquefaction analysis at Wynne Avenue, a peak ground acceleration of 0.51*g*, which was recorded at strong motion station NRG (USC station 3, White Oak Covenant Church, Fig. 1), 1.7 km SE of the study site, was used. Other nearby stations imply ground motions may have been as high as 0.94*g*. At Potrero Canyon, an acceleration of 0.43*g*, which was recorded at strong motion station NWS (USC station 56, Newhall Sun Oil, Fig. 1), 3.8 km east of the study site, was used. The contoured regional map of ground motion by Chang et al. (1996) implies a lower value of 0.35*g* at the study site.

Holocene sediment at Malden Street is nonliquefiable according to the criteria of Seed and Idriss (1982). The sediment has an average clay content >30% and a sensitivity of about 2. Although the writers are inclined to dismiss liquefaction of the Holocene sediment, Mejia (1998) reported field evidence for liquefaction of a clayey silt with a clay content of 24% during the 1989 Loma Prieta earthquake. Neither of the two SPTs in susceptible Pleistocene sediment had factors of safety against liquefaction of less than one [Fig. 9(b)]. However, CPTs suggest that some of the underlying Pleistocene silty sand, unit D, may have shaken strongly enough to have liquefied [Fig. 10(b)]. Most of the sediment that has a factor of safety less than one, as determined from the CPT, lies in a discontinuous 1–2 m thick interval near the Holocene-Pleistocene sedimentary contact.

Limiting Shear Strains

Liquefaction potential and limiting shear strains that were mobilized during the Northridge earthquake also were evaluated with the description of the simplified procedure by Seed et al. (1985). Computations were done with PETAL2 (Chen 1986). To facilitate the comparison of soils with different fines content (f_c), values of $(N_1)_{60}$ were corrected to an equivalent value for clean sand by increasing $(N_1)_{60}$ by $(f_c - 5) \times (7/30)$ (Youd and Idriss 1997). No correction was applied for $f_c < 5\%$ and a constant correction of seven was applied for $f_c > 35\%$.

Large and damaging shear strain is predicted in liquefied Holocene soil during the Northridge earthquake (Fig. 11). By contrast, smaller and generally nondamaging shear strain is predicted in potentially liquefiable Pleistocene soil, which implies that this material did not contribute significantly to ground failure. The liquefaction potential predicted by the original methodology also corroborates the predictions of the modified simplified procedure (Youd and Idriss 1997) that much of the susceptible Holocene soil at the study sites liquefied during the 1994 earthquake.

Strain mobilization may account for the specific location of the down-dropped block at Wynne Avenue. As noted previously, closely spaced CPTs at the site indicate a laterally abrupt fivefold reduction in tip resistance of the upper sand layer, C_1, beneath the south boundary of the down-dropped block. The reduction occurs over a distance of less than 4.5 m, and is caused by an increase in fines content from about 28% to 44%. Larger strains presumably would be mobilized in the part of unit C_1 with lower fines content.

Dynamic Failure of Lean Clay

The nonsusceptibility to liquefaction of Holocene material at the Malden Street site prompted consideration of an alternative mechanism for shallow soil failure. The potential dy-

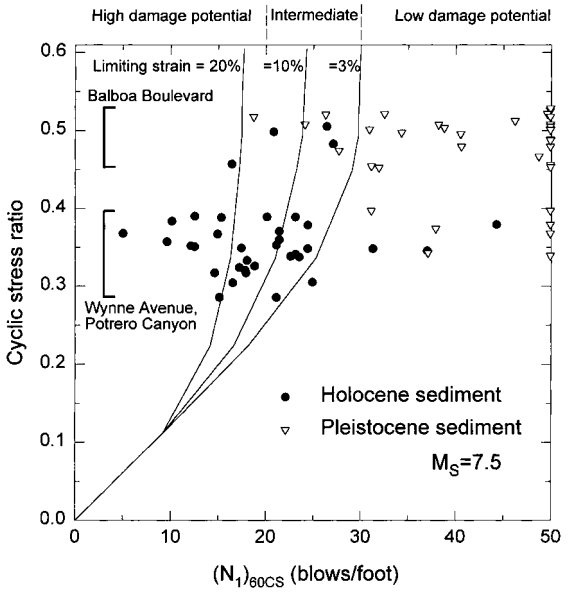

FIG. 11. Liquefaction Potential and Limiting Strains of Holocene and Pleistocene Soil during Northridge Earthquake Based on Relations Proposed by Seed et al. (1985); $(N_1)_{60}$s Were Converted to Equivalent Values for Clean Sand

namic response of the low strength zone between 4.3 and 5.8 m beneath the down-dropped block was of particular interest. To evaluate its seismic stability, the cyclic horizontal shear stress was computed by the formula proposed by Seed and Idriss [1971, Eq. (3)]. Based on the nearest recorded peak ground acceleration of 0.51*g* (station NRG, Fig. 1), the peak cyclic horizontal shear stress was estimated to be twice the 26 kPa in-situ peak shear strength [Fig. 5(a)]. This implies shear failure may have occurred during the main shock. Field shear vane measurements of residual and remolded strengths also indicate that shear failure might lead to a further, although modest, reduction in soil strength and possibly large strains during inertial loading. The sensitivity—the ratio of in-situ measurements of peak to remolded strength—of the lean clay ranges from 1.3 to 2.8.

Ratios of cyclic stress to peak strength also were evaluated at the Wynne Avenue and Potrero Canyon sites; depths to saturated material at Balboa Avenue exceeded the field capability of the vane shear. Ratios commonly reached one at these sites, but in general did not consistently reach the higher values computed at Malden Street.

Dynamic Compaction of Dry Material

In addition to liquefaction-induced deformation of saturated sands, dynamically induced settlements of dry materials at each site were considered. Abdel-Haq and Hryciw (1998) estimated settlements at a site, which was strongly shaken in 1994, in Simi Valley and concluded that about half of the observed settlement resulted from compaction of dry natural material in the upper 3 m. Day (1996) attributed settlements above clayey fill to earthquake-induced compaction during the Northridge earthquake. Soils in the present investigation tend to be silty with fines contents typically exceeding 35%, and in many cases they include high clay contents. Such materials usually are not susceptible to large compaction. Bulk density measurements of selected Shelby tube samples also did not indicate the presence of materials with anomalous low density. Finally, the large horizontal displacements inferred from resurveys at Balboa Boulevard and Malden Street are not consistent with shallow compaction.

Secondary Faulting

Field evidence from investigations at three of the sites, Balboa Boulevard, Wynne Avenue, and Potrero Canyon, is permissive of pre-1994 shallow fault offset beneath parts of the 1994 ground failure zones. Such offset is consistent with the proposal by Cruikshank et al. (1996) and Johnson et al. (1996) that coseismic displacement on nonseismogenic faults—secondary faulting—caused the permanent ground deformation in alluvium during the Northridge earthquake. By their mechanism, soil failure was caused either directly by rupture on the fault or indirectly by large permanent strains above the blind fault.

As noted by Hecker et al. (1995), the belt of ground failure that includes the Balboa Boulevard site coincides with the projection of north-dipping reverse faults within the Mission Hills fault zone. Although stratigraphic and hydrogeologic evidence beneath the south margin of the Balboa Boulevard failure zone is consistent with a pre-1994 fault, the writers were unable to confirm offset or deformation of the contact between the Holocene and Pleistocene sediment at the south margin. This suggests that a fault, if it exists, has not been active during the Holocene. Subsurface evidence for faulting or tectonic deformation beneath the north margin of the Balboa Boulevard failure zone was not found.

The 1.1 m of relief on the buried Pleistocene surface at Wynne Avenue could be either a buried fault scarp or an erosional feature. The relief occurs between borings that are spaced only 4 m apart. If it is a fault, the absence of detectable offset of the two overlying sand lenses implies a low level of activity.

No evidence for a preexisting fault at Malden Street was found. Soil units in the Holocene sediment as well as the contact between Holocene and Pleistocene units were neither deformed nor offset beneath the ground failure.

Observations at Potrero Canyon are inconclusive. Soundings on the south ends of both profiles spanned the zone of ground cracks; access across a stream prevented us from spanning cracks on the north ends. A sandy interval at a depth of 5 m in the eastern profile does not appear to be offset beneath the cracks. However, correlation of units beneath the cracks is uncertain because of the wide spacing of the soundings. Catchings et al. (1998), who conducted seismic reflection profiles adjacent to the geotechnical profiles, infer that the south zone of ground failure overlies a preexisting fault. They conclude, on the basis of the spatial association, that the ground cracking may have resulted from coseismic movement on the preexisting fault.

DISCUSSION

Of the four mechanisms that the writers considered, only shaking-induced soil failure appears likely at all four sites. At three of the sites—Balboa Boulevard, Wynne Avenue, and Potrero Canyon—parts of the Holocene sediment are susceptible to liquefaction, and should have liquefied and mobilized large shear strains at observed levels of ground shaking. At the fourth site—Malden Street—a low-strength lean clay appears to have failed under dynamic loading. The conclusion that permanent ground deformation during the 1994 earthquake was caused by liquefaction of very silty sands is consistent with the experience from the 1971 San Fernando earthquake. Investigators of permanent ground deformation in alluvium concluded that sands with silt contents ranging from 30% to 60% liquefied in 1971 (O'Rourke et al. 1992).

Vented material, which would have provided direct field evidence of liquefaction, may have been absent due to the large depth to, and small thickness of, the liquefied layers. Youd and Garris (1994) reexamined Ishihara's (1985) empirical corre-

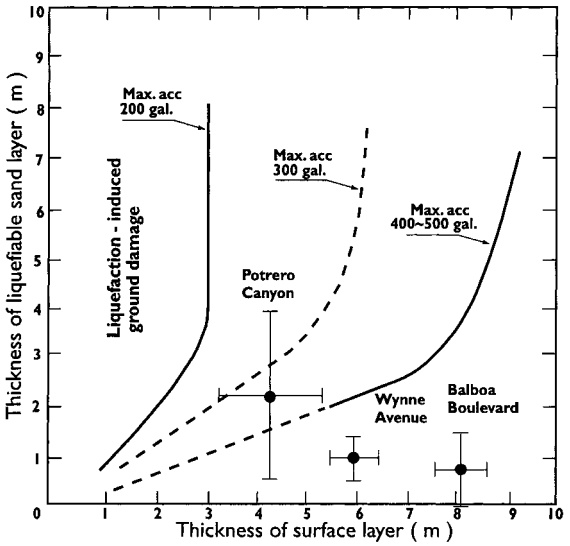

FIG. 12. Comparison of Average Thicknesses ($\pm 1\sigma$) of Holocene Liquefied Material and Surface Layers at Study Sites to Boundary Curves Proposed by Ishihara (1985)

lation of liquefaction-induced surface effects with depth to, and thickness of, the liquefied layer, and concluded that ground cracking without venting of sand boils is more likely as the depth and thickness of the liquefied layer increase and decrease, respectively. The present investigation supports their conclusion. For each site, aggregate thickness of all liquefied Holocene material versus the depth to the top of the shallowest liquefied layer was plotted (Fig. 12). Both the Balboa Boulevard and the Wynne Avenue sites fall outside Ishihara's boundary for the occurrence of surface effects. The Potrero Canyon site, where a few sand boils were observed, plots near the boundary.

The absence of shallow liquefiable material and the presence of a seismically weak lean clay beneath the ground failure at Malden Street is of particular interest. The seismic stability of clays beneath gently sloping ground in alluvial fan environments usually is not evaluated in geotechnical site investigations. The present investigation implies that the seismic stability of these soils should be addressed when high levels of ground shaking are possible. In-situ shear strength measurements may be one method for addressing this problem. Dynamic soil failure also may be a mechanism for nonlinear soil amplification at high shaking levels.

Although the writers cannot dismiss secondary faulting during the Northridge earthquake as the cause of ground deformation, collective consideration of the four study sites does not offer consistent and compelling field evidence of such. Parts of some failure zones may be underlain by pre-1994 faults, but evidence for either tectonic faulting or deformation is not found beneath all of the failures.

Finally, the heterogeneous nature of the alluvial fan sediments and variations in the ground-water table beneath the 1994 ground failures have implications for (1) understanding the spatial distribution of permanent ground deformation; and (2) regional mapping of liquefaction potential. The present investigation documents the significance of variations of local conditions in alluvial fan environments to the specific locations of permanent ground deformation as well as the need to recognize and heed detailed subsurface conditions at a specific site. This heterogeneity of local subsurface conditions may also help to explain localized variations in recorded transient ground motions that are not readily attributable to seismic source and basin effects. In addition, the present study suggests that geologically based regional mapping of areas that are susceptible to liquefaction in alluvial fan environments may be more challenging than in floodplain or fluvial environments. In floodplain environments, detailed surficial geologic mapping can delineate areas that are highly susceptible to liquefaction (Tinsley and Dupré 1992; Holzer et al. 1994). This success presumably derives from the mappable facies associated with the greater continuity and cleanness of fluvial sands relative to alluvial fan deposits. The present investigation suggests that identification of sites that are susceptible to liquefaction is more difficult in alluvial fan deposits derived from fine-grained source rocks. Sands and silts in this environment tend to be clay rich and discontinuous. Delineating areas of saturated Holocene sediment may be the conservative alternative approach for mapping in most alluvial fan settings.

ACKNOWLEDGMENTS

This investigation was partially supported by the National Earthquake Hazards Reduction Program Northridge earthquake supplement to the U.S. Geological Survey. The writers are grateful to the following individuals for assistance: C. Criley, J. J. Butelo, S. Hecker, T. E. Fumal, J. Hamilton, S. Gilstrap, C. C. Conway, and R. E. Kayen. The writers greatly appreciate helpful comments by T. D. O'Rourke and T. L. Youd, who reviewed an early draft of the manuscript, and the anonymous ASCE reviewers.

APPENDIX. REFERENCES

Abdel-Haq, A., and Hryciw, R. D. (1998). ''Ground settlement in Simi Valley following the Northridge earthquake.'' *J. Geotech. and Geoenvir. Engrg.*, ASCE, 124(1), 80–89.

Bennett, M. J., Criley, C., Tinsley, J. C. III, Ponti, D. J., and Holzer, T. L., and Conaway, C. H. (1998). ''Subsurface geotechnical investigations near sites of permanent ground deformation caused by the January 17, 1994 Northridge, California, earthquake.'' *U.S. Geological Survey Open-File Rep. 98-373*, U.S. Geological Survey, Menlo Park, Calif.

Catchings, R. D., Goldman, M. R., Lee, W. H. K., Rymer, M. J., and Ponti, D. J. (1998). ''Faulting apparently related to the 1994 Northridge, California, earthquake and possible co-seismic origin of surface cracks in Potrero Canyon, Los Angeles County, California.'' *Seismological Soc. of America Bull.* 88(6), 1379–1391.

Chang, S. W., Bray, J. D., and Seed, R. B. (1996). ''Engineering implications of ground motions from the Northridge earthquake.'' *Seismological Soc. of America Bull.*, 86(1B), 270–288.

Chen, A. T. F. (1986). ''PETAL2: Penetration testing and liquefaction—An interactive computer program.'' *U.S. Geological Survey Open-File Rep. 86–178*, U.S. Geological Survey, Menlo Park, Calif.

Cruikshank, K. M., Johnson, A. M., Fleming, R. W., and Jones, R. (1996). ''Winnetka deformation zone: Surface expression of coactive slip on a blind fault during the Northridge earthquake sequence, California.'' *U.S. Geological Survey Open-File Rep. 96-698*, U.S. Geological Survey, Denver, Colo.

Day, R. W. (1996). ''Damage due to Northridge earthquake-induced settlement of clayey fill.'' *Envir. and Engrg. Geosci.*, 2(1), 99–105.

Hecker, S., Ponti, D. J., Garvin, C. D., and Hamilton, J. C. (1995). ''Characteristics and origin of ground deformation produced in Granada Hills and Mission Hills during the January 17, 1994 Northridge, California, earthquake.'' The Northridge, California, earthquake of 17 January 1994, M. C. Woods and W. R. Sieple, eds., *California Div. of Mines and Geol. Spec. Publ. 116*, California Division of Mines and Geology, Sacramento, Calif., 111–131.

Holzer, T. L., Bennett, M. J., Tinsley, J. C. III, Ponti, D. J., and Sharp, R. V. (1996). ''Causes of ground failure in alluvium during the Northridge, California, earthquake of January 17, 1994.'' *Proc., 6th U.S.-Japan Workshop on Earthquake Resistant Des. of Lifeline Facilities and Countermeasures for Soil Liquefaction, Tech. Rep. NCEER-96-0012*, National Center for Earthquake Engineering Research, Buffalo, 345–360.

Holzer, T. L., Tinsley, J. C., Bennett, M. J., and Mueller, C. S. (1994). ''Observed and predicted ground deformation—Miller Farm lateral spread, Watsonville, California.'' *Proc., 5th U.S.-Japan Workshop on Earthquake Resistant Des. of Lifeline Facilities and Countermeasures for Soil Liquefaction, Tech. Rep. NCEER-94-0026*, National Center for Earthquake Engineering Research, Buffalo, 79–99.

Ishihara, K. (1985). ''Stability of natural deposits during earthquakes.'' *Proc., 11th Int. Conf. on Soil Mech. and Found Engrg.*, Balkema, Rotterdam, The Netherlands, 321–376.

Johnson, A. M., Fleming, R. M., Cruikshank, K. M., and Packard, R. F.

(1996). ''Coactive fault of the Northridge earthquake—Granada Hills area, California.'' *U.S. Geological Survey Open-File Rep. 96-253*, U.S. Geological Survey, Denver, Colo.

Liquefaction of soils during earthquakes: Committee on Earthquake Engineering. (1985). National Academy Press, Washington, D.C.

''The magnitude 6.7 Northridge, California, earthquake of 17 January 1994.'' *Science*, (1994). 266, 389–397.

Mejia, L. H. (1998). ''Liquefaction at Moss Landing.'' *The Loma Prieta, California, earthquake of October 17, 1989—Liquefaction*, T. L. Holzer, ed., *U.S. Geological Survey Profl. Paper 1551-B*, U.S. Geological Survey, Menlo Park, Calif., B129–B150.

O'Rourke, T. D., Roth, B. L., and Hamada, M. (1992). ''Large ground deformations and their effect on lifeline facilities: 1971 San Fernando earthquake.'' *Case histories of liquefaction and lifeline performance during past earthquakes*, T. D. O'Rourke and M. Hamada, eds., *Tech. Rep. NCEER-92-0002*, National Center for Earthquake Engineering Research, Buffalo, 3-1–3-85.

O'Rourke, T., and Toprak, S. (1997). ''Using GIS to assess water supply damage from the Northridge earthquake.'' *NCEER Bull.*, 11(3), 10–13.

O'Rourke, T. D., Toprak, S., and Sano, Y. (1996). ''Los Angeles water pipeline system response to the 1994 Northridge earthquake.'' *Proc., 6th U.S.-Japan Workshop on Earthquake Resistant Design of Lifeline Facilities and Countermeasures for Soil Liquefaction, Tech. Rep. NCEER-96-0012*, National Center for Earthquake Engineering Research, Buffalo, 1–17.

Pease, J. W., and O'Rourke, T. D. (1997). ''Seismic response of liquefaction sites.'' *J. Geotech. and Geoenvir. Engrg.*, ASCE, 123(1), 37–45.

Rymer, M. J., Fumal, T. E., Schwartz, D. P., Powers, T. J., and Cinti, F. R. (1995). ''Distribution and recurrence of surface fractures in Potrero Canyon associated with the 1994 Northridge, California, earthquake.'' *The Northridge, California, earthquake of 17 January 1994*, M. C. Woods and W. R. Seiple, eds., *California Div. of Mines and Geol. Spec. Publ. 116*, California Division of Mines and Geology, Sacramento, Calif., 133–146.

Seed, H. B., and Idriss, I. M. (1971). ''Simplified procedure for evaluating soil liquefaction potential.'' *J. Soil Mech. and Found. Div.*, ASCE, 97(9), 1249–1273.

Seed, H. B., and Idriss, I. M. (1983). ''Ground motions and soil liquefaction during earthquakes.'' *Earthquake Engrg. Res. Inst. Monograph*, Earthquake Engineering Research Institute, El Cerrito, Calif.

Seed, H. B., Tokimatsu, K., Harder. L. F., and Chung, R. M. (1985). ''Influence of SPT procedures in soil liquefaction resistance investigations.'' *J. Geotech. Engrg.*, ASCE, 111(12), 1425–1445.

Standard method for field vane shear test in cohesive soil. (1983). *Annual book of ASTM standards*, Vol. 4.08: Soil and rock; building stones. ASTM, West Conshohoken, Pa., 404–407.

Stewart, J. P., Seed, R. B., and Bray, J. D. (1996). ''Incidents of ground failure from the 1994 Northridge earthquake.'' *Seismological Soc. of America Bull.*, 86(1B), 300–318.

Tinsley, J. C. III, and Dupré, W. R. (1992). ''Liquefaction hazard mapping, depositional facies, and lateral spreading ground failure in the Monterey Bay area during the 10/17/89 Loma Prieta earthquake.'' *Proc., 4th U.S.-Japan Workshop on Earthquake Resistant Des. of Lifeline Facilities and Countermeasures for Soil Liquefaction, Tech. Rep. NCEER-92-0019*, National Center for Earthquake Engineering Research, Buffalo, 71–85.

''USGS response to an urban earthquake, Northridge '94.'' (1996). *U.S. Geological Survey Open-File Rep. 96-263*, U.S. Geological Survey, Menlo Park, Calif.

Wentworth, C. M., and Yerkes, R. F. (1971). ''Geologic setting and activity of faults in the San Fernando area, California.'' *The San Fernando, California, earthquake of February 9, 1971. U.S. Geological Survey Profl. Paper 733*, U.S. Geological Survey, Menlo Park, Calif., 6–16.

Youd, T. L., and Garris, C. T. (1994). ''Liquefaction-induced ground surface disruption.'' *Proc., 5th U.S.-Japan Workshop on Earthquake Resistant Des. of Lifeline Facilities and Countermeasures for Soil Liquefaction, Tech. Rep. NCEER-94-0026*, National Center for Earthquake Engineering Research, Buffalo, 27–40.

Youd, T. L., and Idriss, I. M., eds. (1997). ''NCEER workshop on evaluation of liquefaction resistance of soils.'' *Tech. Rep. NCEER-97-0022*, National Center for Earthquake Engineering Research, Buffalo.